J|A|C|S
COMMUNICATIONS

Published on Web 03/13/2008

Engineering Strength, Porosity, and Emission Intensity of Nanostructured CdSe Networks by Altering the Building-Block Shape

Hongtao Yu,[†] Robert Bellair,[‡] Rangaramanujam M. Kannan,[‡] and Stephanie L. Brock*,[†]

Department of Chemistry and, Department of Chemical Engineering and Materials Science, Wayne State University, Detroit, Michigan 48202

Received February 18, 2008; E-mail: sbrock@chem.wayne.edu

Semiconducting nanoparticles have the potential to revolutionize many traditional technologies and, as such, have received considerable attention from the scientific community. In the past five years, the priority of semiconducting nanoparticle research has shifted from studies of size and shape dependent electro-optical properties to designing more complex nanostructures[1,2] and assembling simple nanometer-scale building blocks into functional architectures.[3,4] Recently, our laboratory successfully developed a general methodology to assemble quantum dots (spherical semiconducting nanoparticles) into 3-D porous networks without the presence of intervening ligands that can moderate dot−dot interactions.[5] Experimental data suggest that the resultant assemblies maintain the crystalline phase and quantum confinement of the building blocks and exhibit a colloidal morphology similar to that of a base-catalyzed silica aerogel.[6] While the quantum dot aerogels exhibit relatively high surface areas ($\geq$100 m^2/g) and are mesoporous, making them suitable for catalytic and sensing applications, the monolithic structures are fragile and the native luminescent intensity is weak. Here we show that the inherent properties of the metal chalcogenide aerogel framework can be enhanced just by changing the shape of the building block from which it is assembled. Thus, quantum rods of CdSe assemble to form a different inherent morphology than spherical CdSe quantum dots, and the resultant rod-based aerogels show augmented gel strength, surface area, and band-edge luminescence intensity.

Highly monodisperse CdSe nanodots and nanorods were synthesized by modification of a literature method[7] and surface modified with thiolate ligands by treatment with 11-mercaptoundecanoic acid (MUA) in the presence of tetramethylammonium hydroxide. Subsequent oxidative removal of the surface thiolate ligands by treatment with tetranitromethane led to gel formation, concomitant with production of the disulfide of MUA as a byproduct. Solvent exchange and supercritical CO_2 drying yielded aerogel monoliths.

TEM images (Figure 1) demonstrate the different building blocks and the morphology of the resultant aerogels. The CdSe rod aerogel exhibits a unique morphology relative to the colloidal-type dot aerogel, and is similar to an acid-catalyzed silica aerogel with a polymer-type framework.[8] The rods appear to form interpenetrating "struts" (Figure 1d) that are connected preferentially at their apexes due to the higher surface free energy (attributed to the presence of more dangling bonds) of apical facets relative to axial facets.[9,10] High resolution TEM images, along with selected area electron diffraction, reveal a high degree of crystallinity (Figure 1c,d), and the lattice fringes and diffraction rings can all be indexed to hexagonal CdSe. These data are consistent with powder X-ray diffraction patterns collected on bulk aerogel samples.

Surface area and porosity analyses were conducted using nitrogen physisorption measurements performed at 77 K on powder aerogel samples. The data (Table 1) show that the CdSe rod aerogels exhibit over twice the surface area and cumulative pore volume of the dot aerogels. Since the average pore diameter is slightly smaller for the rod aerogels, this implies a larger number of accessible pores in the rod aerogels relative to the dot aerogels. This is an unexpected observation, since, in silica aerogels, it is the colloidal aerogel (base-catalyzed) that exhibits the higher surface area relative to the polymeric aerogel (acid-catalyzed) and the surface area scales with the average pore size.[11] We attribute the high surface areas of the CdSe polymeric aerogels in part to the strength of the rod-network, which enables the pore volume to be maintained during aging and drying processes. Consistent with this hypothesis, the rod gels show a decreased tendency toward syneresis, in which the gel becomes more compact and exudes solvent, relative to dot gels. Thus, rod gels hold their shape upon inversion (Figure 2, insets).

To quantify some of the structural attributes of the gel framework, oscillatory shear linear viscoelastic property measurements were conducted on aerogel−polydimethylsiloxane (PDMS) composites (5 wt % CdSe). Rheology is sensitive to structural changes in particle networks (even at 0.5 wt % particles), as reflected in their reinforcement of a polymer matrix, and is often employed to elucidate structure–property relationships in nanostructured materials.[12] In the present case, since PDMS-filler interactions are anticipated to be weak, any viscosity enhancements in the aerogel-PDMS composites are expected to be reflective of the strength of the aerogel network. The magnitude of the complex viscosity of the aerogel-PDMS composites, Figure 2, reveals a clear difference in reinforcement between the network morphologies. The viscosity enhancement (at 0.01 r/s) is nearly 100% for the rod aerogel, double that obtained from the dot aerogel. Furthermore, the rod aerogel shows a nonzero slope at low frequencies, indicative of a "percolated" network in filled polymer systems. The difference in enhancement for rod aerogels versus dot aerogels does not appear to be due to structural attributes of the building blocks themselves, since PDMS composites formed from discrete dots and rods show identical behavior (~20% enhancement over PDMS). Thus, our results suggest that the aerogels composed from rod-shaped nanoparticles have greater network strength than those created from dot-shaped nanoparticles. These observations are consistent with those of Leventis, who has noted that polymer-cross-linked aerogels based on anisotropic structures, such as the interpenetrating aerogel morphology created from "worm-like" vanadia, can have dramatically increased mechanical strengths relative to colloidal aerogels.[13]

[†] Department of Chemistry.
[‡] Department of Chemical Engineering and Materials Science.

10.1021/ja801212e CCC: $40.75

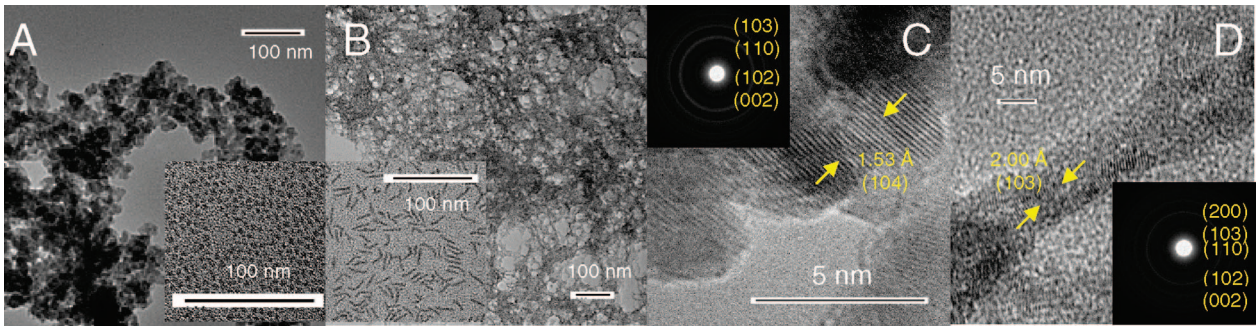

Figure 1. TEM images of CdSe colloidal aerogels (A) and polymeric aerogels (B) and their building blocks (dots and rods, inset). High resolution images show lattice fringes in the dot (C) and rod assemblies (D); the presence of nanorod "struts" is clearly present in the latter. The insets show selected area electron diffraction patterns; the diffraction rings (inner to outer) can be indexed to hexagonal CdSe crystal planes (bottom to top).

Table 1. Brunauer–Emmett–Teller (BET) Surface Areas, Barrett–Joyner–Halenda (BJH) Absorption Average Pore Diameters and BJH Cumulative Pore Volumes of CdSe Colloidal and Polymeric Aerogels (Average of Three Independent Samples); Primary Particle Size, and Optical Bandgap of the Building Block and Aerogel

CdSe aerogel	BET surface area (m^2/g)	average pore diameter (nm)	cumulative pore volume (cm^3/g)	size of building block (nm)	absorption onset value: primary particle/ aerogel (eV)
colloidal	107 ± 10	35.4 ± 2.4	0.59 ± 0.31	(dot) 3.17 ± 0.31	2.15/2.12
polymeric	239 ± 7	24.9 ± 1.5	1.64 ± 0.11	(rod) $3.40 \pm 0.33 \times 22.7 \pm 2.2$	2.06/2.02

Optical absorption and emission measurements reveal that both types of CdSe aerogel maintain a similar degree of quantum confinement to that of the respective building block from which they were assembled. This is manifest in a nearly identical band gap value (Table 1) for the primary particles and aerogels. More impressively, the CdSe rod aerogel monolith shows a band edge emission peak that is 25 times more intense than a dot aerogel monolith with the same mass (Figure 3, ratio of the emission maximum intensities), despite the fact that the primary particles (rods and dots) have comparable emission intensities when compared on a per gram basis. While the specific origin of this effect is still under investigation, the extreme differences in emissivity between colloidal dot and polymeric rod aerogels underscore the key finding of this report: altering the shape of the building block from which nanostructured networks are assembled is an effective way to tune the basic properties of metal chalcogenide semiconducting aerogels.

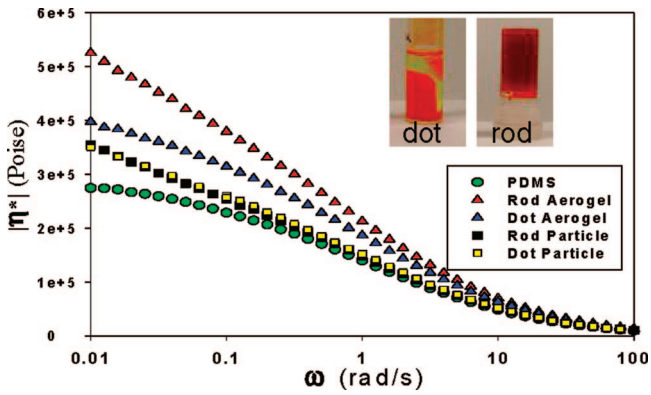

Figure 2. Complex viscosity data for PDMS and PDMS composites of dots, rods, and corresponding aerogels (5 wt % CdSe). The insets show the effect of syneresis on shrinkage of dot gels relative to rod gels.

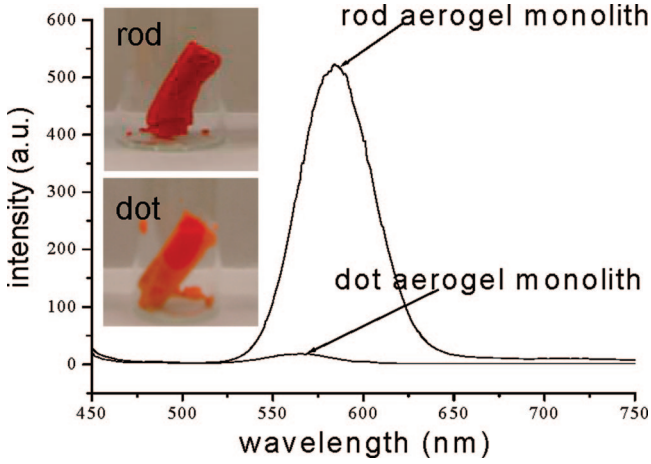

Figure 3. Graph of room temperature emission spectra ($\lambda_{ex} = 440$ nm) of CdSe dot and rod aerogel monoliths (pictured in insets) with the same mass (dot, 0.0183 g; rod, 0.0181 g).

Acknowledgment. We thank Dr. Yi Liu for assistance with TEM measurements. This work was supported in part by the Donors of the Petroleum Research Fund (AC-43550), NSF (DMR-0701161, DMR-0216084), and the Institute of Manufacturing Research (WSU).

Supporting Information Available: Synthesis and characterization details. This material is available free of charge via the Internet at http://pubs.acs.org.

References

(1) Milliron, D. J.; Hughes, S. M.; Cui, Y.; Manna, L.; Li, J.; Wang, L.-W.; Alivisatos, P. A. *Nature* **2004**, *430*, 190–195.
(2) Robinson, R. D.; Sadtler, B.; Demchenko, D. O.; Erdonmez, C. K.; Wang, L.-W.; Alivisatos, P. A. *Science* **2007**, *317*, 355–358.
(3) Shevchenko, E. V.; Talapin, D. V.; Kotov, N. A.; O'Brien, S.; Murray, C. B. *Nature* **2006**, *439*, 55–59.
(4) Tang, Z.; Zhang, Z.; Wang, Y.; Glotzer, S. C.; Kotov, N. A. *Science* **2006**, *314*, 274–278.
(5) Mohanan, J. L.; Arachchige, I. U.; Brock, S. L. *Science* **2005**, *307*, 397–400.
(6) Arachchige, I. U.; Brock, S. L. *J. Am. Chem. Soc.* **2006**, *128*, 7964–7971.
(7) Peng, Z. A. P.; Peng, X. *J. Am. Chem. Soc.* **2001**, *123*, 183–184.
(8) Hüsing, N.; Schubert, U. *Angew. Chem., Int. Ed.* **1998**, *37*, 22–45.
(9) Halpert, J. E.; Porter, V. J.; Zimmer, J. P.; Bawendi, M. G. *J. Am. Chem. Soc.* **2006**, *128*, 12590–12591.
(10) Mokari, T.; Rothenberg, E.; Popov, I.; Costi, R.; Banin, U. *Science* **2004**, *304*, 1787–1790.
(11) Anderson, M. L.; Morris, C. A.; Stroud, R. M.; Merzbacher, C. I.; Rolison, D. R. *Langmuir* **1999**, *15*, 674–681.
(12) Kharchenko, S. B.; Douglas, J. F.; Obrzut, J.; Grulke, E. A.; Migler, K. B. *Nat. Mater.* **2004**, *3*, 564–568.
(13) Leventis, N. *Acc. Chem. Res.* **2007**, *40*, 874–884.

JA801212E